CHAPTER-5

ELECTRON ACCELERATION TO GEV ENERGY BY A CHIRPED LASER PULSE IN VACUUM IN THE PRESENCE OF AZIMUTHAL MAGNETIC FIELD

5.1 INTRODUCTION

The theoretical and experimental studies of electron acceleration by laser have been fascinating and fast growing field of research for last few decades [13, 45, 57, 70, 105]. These studies explore the techniques for the higher energy gains by electron through laser pulse in vacuum and plasmas. Malka *et al.* [13] reported experimentally the vacuum acceleration of electrons. They observed elctron energy gain of the order of MeV through a high-intensity short pulse laser pulse ($10^{19} W/cm^2$, $300 fs$). High quality electron beams were observed by Geddes *et al.* [45] from a laser wakefield accelerator with a plasma channel guiding. They proposed peak energy in simulation of about $200 MeV$ which is close to experimental results. An electron in vacuum may be accelerated by the laser field directly. A planar-laser pulse cannot be employed for electron acceleration, because it overtakes an electron the latter is ponderomotively driven forwards in the raising part, but then backwards in trailing part, resulting in no net gain by the electron [20]. An electron can gain a significant amount of enrgy and retain it with an applied magnetic field of suitable magnitude and period. The magnetic field strengthens the cyclotron oscillations due to $\vec{v} \times \vec{B}$ force. Hence contributes significantly towards forward drift and energy gain of electron. The electron energy gain of $1.2 GeV$ was obtained [64] with an intense laser pulse peak intensity of $8 \times 10^{21} W/cm^2$. The characteristics variations in polarizations of laser pulse were studied to investigate the betterment in interaction of laser pulse with electron for high energy gain [55, 66, 96]. Sohbatzadeh and Aku [96] proposed that the CP laser pulse is more efficient in electron bunch acceleration in comparison to elliptical and linear polarizations. The pulse parameters of interaction with electrons are time averaged with circular polarization which increases the interaction of laser pulse with electrons. Gupta *et al.* [66] observed the electron energy gain of $1.5 GeV$ with a radially polarized laser pulse with a magnetic field of about $1MG$. After attaining the maximum energy gain, the electron gets decelerated, losses energy and tends to go out of phase with respect to the field even with high intensity laser pulse. A pre-accelerated electron was employed to enforce a confined trajectory for longer duration [55] with a CP laser pulse. Thus electron injection is easier in vacuum with a pre-accelerated electron than that in plasmas. Khachatryan *et al.* [46] evaluated the transverse and longitudinal momentum dynamics for the charged particles during interaction with a chirped electromagnetic pulse and obtained final longitudinal momentum corresponding to energy $8.55MeV$ for electron acceleration with linearly chirped pulse. Liu *et al.* [58] investigated the role of intense linearly polarized (LP) laser pulse in collimation and acceleration of relativistic electron beams in plasma. An azimuthal magnetic field of about $100MG$ was observed to be self-generated during laser plasma interaction. They stated that the additional acceleration is the result of laser-magnetic resonance acceleration (LMRA) around the peak of the azimuthal magnetic field. The interaction of relativistic strong laser pulses with electron along with hundreds of MG azimuthal quasi-static magnetic field is a complex process and a manipulation of $100MG$ magnetic field may not be easy in plasma. The resonant enhancement of electron energy was obtained with a frequency chirped plane polarized laser pulse in an azimuthal magnetic field in plasma [73] and concluded that the magnetic field for which resonance occurs increases with plasma density. Such increasing magnetic field can be neglected in vacuum. Vacuum acceleration has some advantages over plasma as laser posses higher group velocity and the plasma instabilities are absent in vacuum which provides a better platform for electron laser interaction in vacuum than plasma. Hartemann *et al.* [17] compared the energy in the drive laser pulse to the kinetic energy acquired by $1nC$ electron bunch in the inverse free electron laser and found the energy transferred to the beam is 16.6% of the chirped pulse laser energy. However, they proposed a compact vacuum laser accelerator capable of accelerating picosecond electron bunches with a high gradient of about GeV/m and very low energy spread. Afhami and Eslami [117] have analysed the plasma wake field generation by the effect of nonlinear chirped Gaussian laser pulse. They considered different types of chirped pulse with linear, nonlinear and periodic characteristics to evaluate the wake field excitation behind the laser pulse. The more oscillation of the main pulse leads to decreasing behaviour of wake field generation. The characteristic variation frequency chirp like linear and quadratic chirp further improves the energy gain [46, 49]. Galow *et al.* [108] proposed a scheme for vacuum autoresonance laser acceleration (ALA) by a CP laser pulse in the presence of axial magnetic field. They observed an acceleration gradient of above $2.2GeV/m$ with laser peak intensity of about $10^{18} W/cm^2$ (peak power $\sim 10PW$) and axial magnetic field strength of about $60T$.

In this chapter we present the results of a relativistic 3D single particle code for electron acceleration by a CP chirped laser pulse in the presence of an azimuthal magnetic field in vacuum. In comparison to the model presented by Galow *et al.* [108], we have employed the azimuthal magnetic field in place of axial magnetic field and observe the electron acceleration at comparatively low values of magnetic field. Additionally, we have examined the effect of linear chirp for electron acceleration by CP laser pulse in vacuum. The efficiency of energy transfer in CP laser pulse is higher than that in case of LP laser pulse. For an appropriate position of the peak of the laser pulse, the ponderomotive force due to the laser pushes the electron forward and electron get accelerated rapidly. The linear frequency chirp increases the duration of interaction of laser pulse with electron which maintains the resonance for longer duration. The azimuthal magnetic field having pinching effect which keeps the motion of electron along the direction of propagation for larger distances. Hence, the electron not only gains much higher energy at resonance with optimum values of the magnetic field but also retains the high energy for larger distance even after passing of the laser pulse. Using a pre-accelerated electron of few MeV of initial energy an energy gain of the order of GeV is observed in the presence of relatively smaller azimuthal magnetic field of the order of $100kG$ with a linearly CP chirped laser pulse of relatively smaller intensities in vacuum.

We examine the electron dynamics under influence of an azimuthal magnetic field with a frequency chirped CP laser in vacuum in section 5.2. We solve numerically the coupled differential equations and use a simulation code to find the electron trajectory and energy in vacuum. We discuss the numerical results in section 5.4. A conclusion of results is given in section 5.5.

5.2 FIELD DISTRIBUTION FOR CIRCULARLY POLARIZED CHIRPED LASER PULSE

We consider a CP chirped laser pulse propagating along the z-direction with transverse components of electric field ($\vec{E} = \hat{x}E_x + \hat{y}E_y$) given as:

$$E_x = \frac{E_0}{f}\sin(\phi)\exp\left(-\frac{(\xi-\xi_0)^2}{\sigma^2} - \frac{r^2}{r_0^2 f^2}\right), \tag{5.1}$$

$$E_y = \frac{E_0}{f}\cos(\phi)\exp\left(-\frac{(\xi-\xi_0)^2}{\sigma^2} - \frac{r^2}{r_0^2 f^2}\right), \tag{5.2}$$

where $\phi = k(\xi)\xi + \tan^{-1}(z/Z_R) - zr^2/(Z_R r_0^2 f^2) + \phi_0$, $f^2 = 1 + (z/Z_R)^2$, $k(\xi) = \omega(\xi)/c$ is the wave number, $\omega(\xi)$ is an arbitrary frequency chirp and is equal to $\omega_0(1+\alpha\xi)$ for linear [117] and negative chirp, α is the frequency chirp parameter, $Z_R = kr_0^2/2$ is the Rayleigh length, $\xi = z - ct$ is the retarded coordinate, ϕ_0 is the initial phase, σ is the pulse length, $r^2 = x^2 + y^2$, r_0 is minimum laser spot size, ω_0 is the laser frequency, ξ_0 is the initial position of the pulse peak, and c is the velocity of light in vacuum. The laser spot size r_0 is assumed to be same for all frequency components. The spatial variations of field in transverse direction give rise to a longitudinal field component. The longitudinal component of electric field is obtained as $E_z = -(i/k)(\partial E_x/\partial x + \partial E_y/\partial y)$. The longitudinal component is smaller by a factor of $(1/k)$ compared to dominant transverse field components. Thus we have neglected the longitudinal component of electric field because of very small amplitude in comparison with transverse component [64]. The magnetic field components of the laser pulse can be obtained through Maxwell's equations and expressed as:

$$\vec{B} = -ic\frac{\vec{\nabla}\times\vec{E}}{\omega(\xi)}. \tag{5.3}$$

The laser pulse imparts energy to the electron that carries current in the z-direction and experiences an azimuthal magnetic field. Liu *et al.* [58] observed a self-generated azimuthal magnetic field of about $100MG$ during laser plasma interaction. Such self-generated field is feasible to apply from external source in vacuum. Takakura *et al.* [93] have proposed a model for generation of azimuthal magnetic field. This externally applied azimuthal magnetic field [27, 73] is expressed as:

$$\vec{B}_\theta = (y\hat{x} - x\hat{y})\frac{B_0}{r_0}\exp\left(-\frac{r^2}{r_0^2}\right), \tag{5.4}$$

where the constant B_0 represents the maximum amplitude of magnetic field. The azimuthal magnetic field rises from zero at $r = 0$ to a maximum around $r \sim r_0$. Figure 5.1 shows a schematic of vacuum acceleration of electron by a CP chirped laser pulse with an azimuthal magnetic field.

5.3 ELECTRON DYNAMICS AND RELATIVISTIC ANALYSIS

The equations representing the electron momentum and energy are:

$$\frac{dp_x}{dt} = -eE_x + e\beta_z B_y + e\beta_z B_{\theta y}, \tag{5.5}$$

$$\frac{dp_y}{dt} = -eE_y - e\beta_z B_x - e\beta_z B_{\theta x}, \tag{5.6}$$

$$\frac{dp_z}{dt} = -e(\beta_x B_y - \beta_y B_x) - e(\beta_x B_{\theta y} - \beta_y B_{\theta x}), \tag{5.7}$$

$$\frac{d\gamma}{dt} = -e(\beta_x E_x + \beta_y E_y), \tag{5.8}$$

where p_x, p_y and p_z are x, y and z components of the momentum $\vec{p} = \gamma m_0 \vec{v}$ respectively; β_x, β_y and β_z are x, y and z components of the normalized velocity $\vec{\beta} = \vec{v}/c$ respectively; $\gamma^2 = 1 + (p_x^2 + p_y^2 + p_z^2)/(m_0 c)^2$ is the Lorentz factor, $-e$ and m_0 are the charge and rest mass of electron respectively.

The following are the normalized parameters:

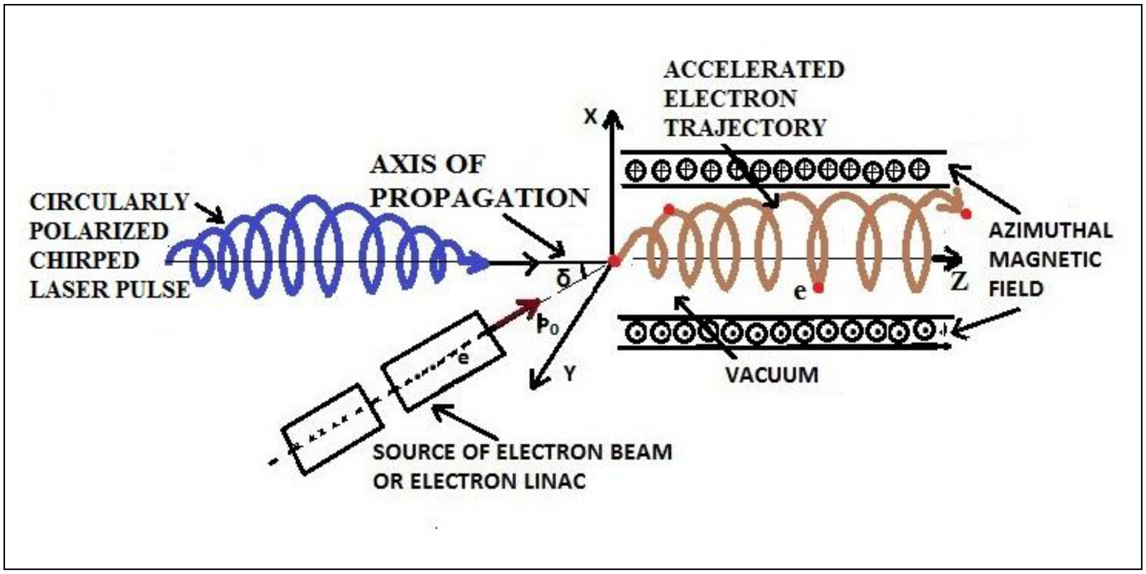

Figure 5.1. A schematic showing the vacuum acceleration of electron by a CP chirped laser pulse with an azimuthal magnetic field.

$a_0 \to \frac{eE_0}{m_0\omega_0 c}$, $\tau \to \omega_0 t$, $\sigma' \to \frac{\omega_0 \sigma}{c}$, $r_0' \to \frac{\omega_0 r_0}{c}$, $z_0' \to \frac{\omega_0 z_0}{c}$, $x' \to \frac{\omega_0 x}{c}$, $y' \to \frac{\omega_0 y}{c}$,

$z' \to \frac{\omega_0 z}{c}$, $\beta_x \to \frac{v_x}{c}$, $\beta_y \to \frac{v_y}{c}$, $\beta_z \to \frac{v_z}{c}$, $p_0' \to \frac{p_0}{m_0 c}$, $p_x' \to \frac{p_x}{m_0 c}$, $p_y' \to \frac{p_y}{m_0 c}$,

$p_z' \to \frac{p_z}{m_0 c}$, $k_0' \to \frac{ck_0}{\omega_0}$, $\alpha' \to \frac{\alpha c}{\omega_0}$, and $b_0 \to \frac{eB_0}{m_0\omega_0 c}$.

Equations (5.5)-(5.8) are the coupled ordinary differential equations. We solve these equations numerically for electron trajectory and energy.

We consider that the electron is initially injected [55] at a small angle δ to the direction parallel to propagation of laser pulse with $\vec{p}_0 = \hat{x} p_0 \sin\delta + \hat{z} p_0 \cos\delta$ where p_0 is the initial momentum of the electron.

5.4 RESULTS AND DISCUSSION

We have chosen the following dimensionless parameters for numerical analysis: $a_0 = 2.5$ (corresponding to laser intensity $I \sim 1.7\times10^{19}\ W/cm^2$), $a_0 = 5$ (corresponding to laser intensity $I \sim 6.92\times10^{19}\ W/cm^2$) and $a_0 = 10$ (corresponding to laser intensity

$I \sim 2.74\times10^{20}\ W/cm^2$) with wave length $\lambda_0 \sim 1\mu m$; $r_0' = 900$ (corresponding to laser spot sizes $r_0 \sim 151\mu m$); and $p_0' = 1$, 1.5, 2 and 2.5; $\sigma' = 70$ (corresponding to laser pulse duration of $200 fs$); $\delta = 10^\circ$; $\phi_0 = 0$; $b_0 = 0.0005$ (corresponding to a magnetic field of $53 kG$), $b_0 = 0.001$ (corresponding to a magnetic field of $106 kG$) and $b_0 = 0.005$ (corresponding to a magnetic field of $534 kG$); and $z_0' = -300$.

Figure 5.2, shows the electron trajectory in three dimensional planes in the absence and presence of chirping. The electron rotates around the direction of propagation of laser pulse during interaction with laser pulse in the presence of magnetic field. The magnetic field enhances the strength of $\vec{v}\times\vec{B}$ force. Gupta and Ryu [55] proposed that the electron traverse more distance along the direction parallel to propagation of laser pulse in the presence of obliquely incident magnetic field with normalized values $b_0 = 0.1$ and 0.01. In the absence of chirping the electron after attaining the maximum energy gain, retains the gain till saturation of betatron resonances. Afterward, it is decelerated slowly with decrease in radius as appearing in fig. 5.2(a). The frequency chirped laser pulse supports better interaction between the laser and the electron. It enforces a very small divergence in electron trajectory as appearing in fig. 5.2(b). Hence, it maintains the resonance for longer durations. The combined effect of chirping and pinching supports the resonant enhancement of higher energy gains for relatively larger distances.

Figure 5.3, shows the variation of energy gain γ with normalized magnetic field b_0. In fig. 5.3(a) and 5.3(b), electron energy gain has been analysed at different values of normalized initial momentum with and without chirping for $a_0 = 2.5$ and 5 respectively. Higher energy gain appears with chirped laser pulse than that with unchirped laser pulse in the presence of azimuthal magnetic field. As depicted from fig. 5.3(a) for $a_0 = 2.5$ and $p_0' = 1.5$, the energy gain is $\gamma = 1042$ in the presence of chirp factor $\alpha' = 0.0015$ which is about 65% higher than that of $\gamma = 630$ in the absence of chirping. In fig 5.3(b), for $a_0 = 5$ and $p_0' = 1.5$ the electron energy gain is $\gamma = 3111$ in the presence of chirp factor $\alpha' = 0.0011$ which is 18% higher than that of $\gamma = 2632$ in the absence of chirping. This is

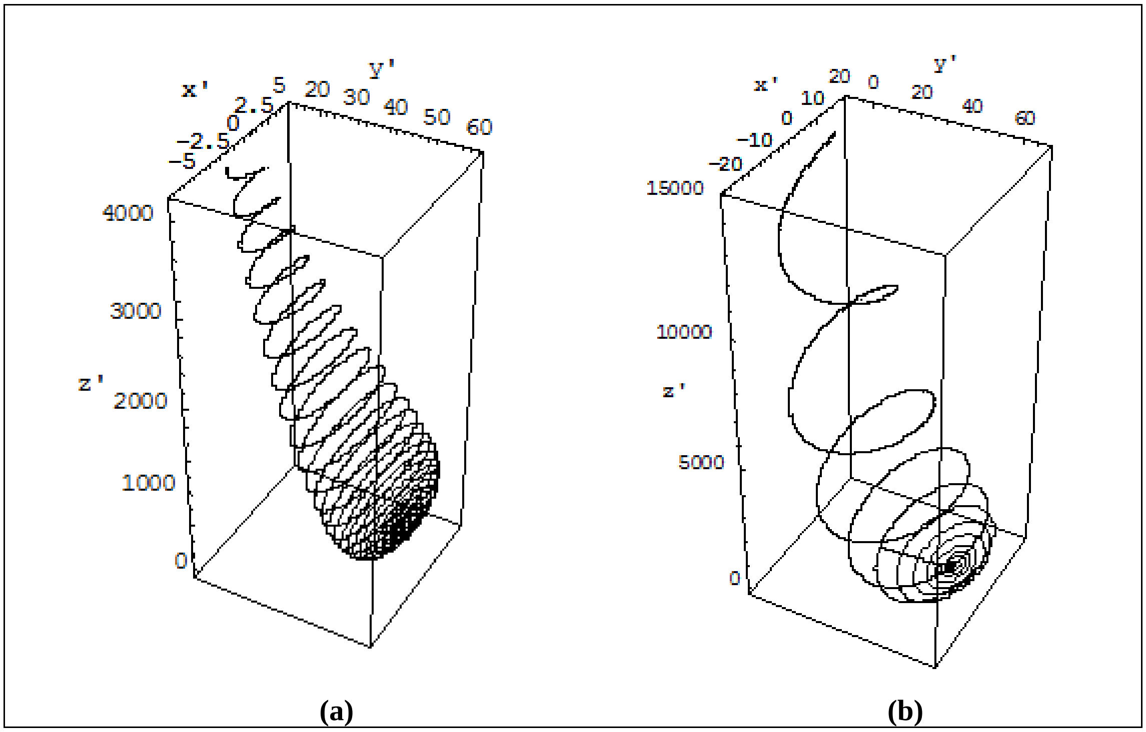

Figure 5.2. Electron trajectory in 3D plane without and with chirping for CP laser pulse at $a_0 = 2.5$, $b_0 = 0.005$ and $p_0' = 1$. (a) $\alpha' = 0$ and (b) $\alpha' = 0.003$. The other parameters are $r_0' = 900$, $\sigma' = 70$, $\phi_0 = 0$, $\delta = 10^\circ$ and $z_0' = -300$.

the minimum predicted energy gain with a set of parameters. For such energy gain the value of optimum magnetic field is taken as $b_0 = 0.00165$ (corresponding to $176kG$) in the presence of chirping which is 60% smaller than $b_0 = 0.005$ (corresponding to $534kG$) to achieve a high energy gain in the absence of chirping. The normalized initial momentum is optimized for high energy gain. The high energy gain for $a_0 = 2.5$ appears with $p_0' = 2.5$ whereas for $a_0 = 5$ it appears with $p_0' = 1.5$. This is because the acceleration gradient decreases with initial momentum and increases with laser pulse intensity. Thus with higher values of intensity, the optimum value of initial momentum for high energy gain appears to be small and vice versa. Fig. 5.3(c) shows the variation of energy gain γ with b_0 for different values of laser pulse intensity parameters $a_0 = 6$, 7.5, 10, 12.5, 15

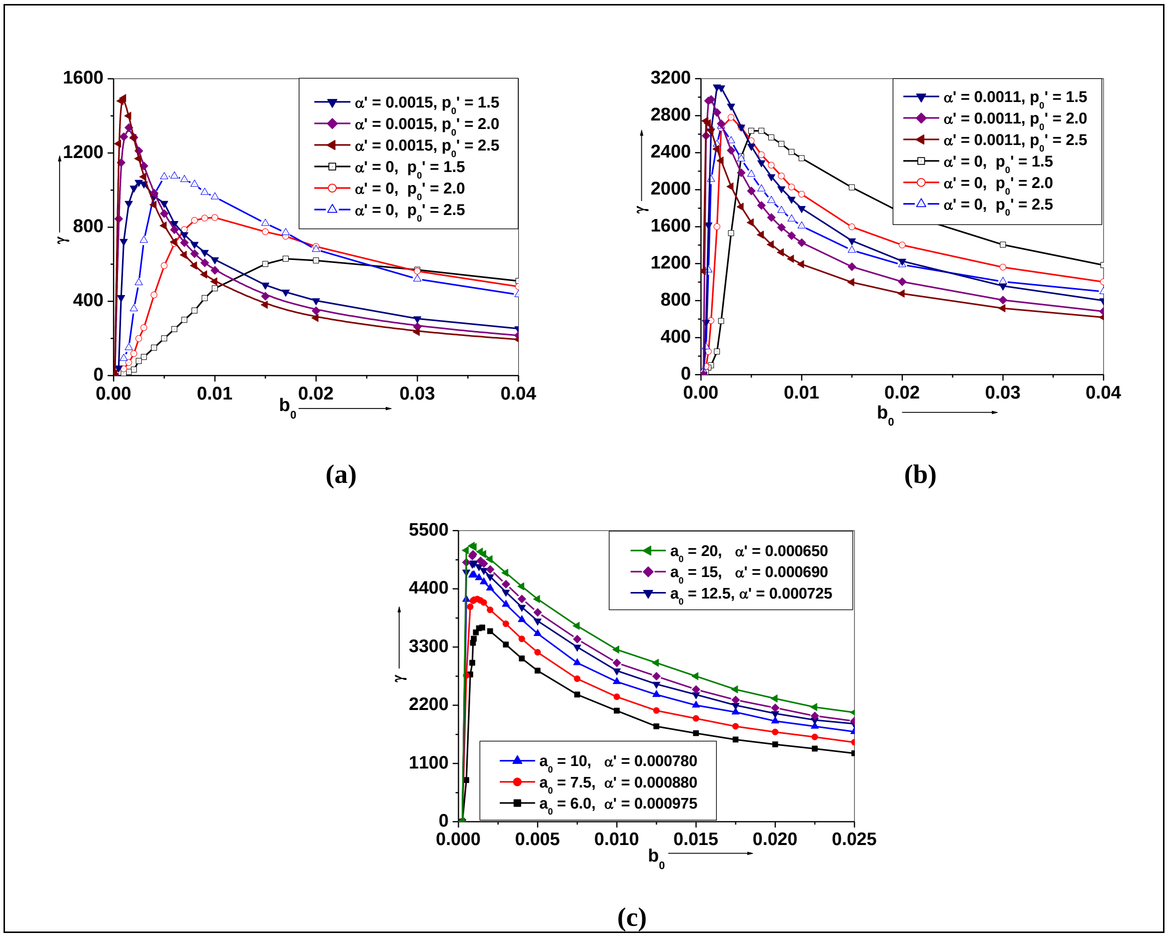

Figure 5.3. Energy gain γ with normalized magnetic field b_0 for different values of normalized initial momentum and intensity parameters for CP laser pulses. (a) $p_0'=1.5$, 2, **and** 2.5 **at** $a_0=2.5$ **with** $\alpha'=0$ **and** $\alpha'=0.0015$, **(b)** $p_0'=1.5$, 2, **and** 2.5 **at** $a_0=5$ **with** $\alpha'=0$ **and** $\alpha'=0.0011$, **and (c)** $a_0=6$, 7.5, 10, 12.5, 15, **and** 20 **at** $p_0'=1.5$ **with** $\alpha'=0.000975$, 0.00088, 0.00078, 0.000725, 0.00069, **and** 0.00065 **respectively. Rest parameters are same as taken in fig. 5.2.**

and 20 at $p_0=1.5$ and suitable values of chirp factor. In order to obtain high energy gain the optimum value of magnetic field remains small with higher values of laser pulse intensity. After attaining maximum gain at resonance the electron energy decreases and almost saturates for the larger values of magnetic field. The optimum value of magnetic field corresponding to laser pulse intensity for the maximum energy gain appears with optimized chirp parameter. The energy gain increases with laser pulse intensity. For $a_0 = 20$, the energy gain $\gamma = 5210$ appears at $b_0 = 0.000875$ which is higher than $\gamma = 5052$ for $a_0 = 15$ at $b_0 = 0.0009$ with $p_0' = 1.5$. The appeared values of normalized magnetic field for high energy gain are feasible and can be produced experimentally [94, 115].

Figure 5.4 shows the variation of electron energy gain γ as a function of the normalized distance z'. In fig. 5.4(a) and 5.4(b), we see the variation of γ with z' in the absence and presence of chirping for different values of normalized momentum $p_0' = 1.5$, 2, and 2.5 with optimum values of magnetic field for $a_0 = 2.5$ and $a_0 = 5$ respectively. A pre-accelerated electron has sufficient kinetic energy to gain high energy during acceleration. Additionally the applied magnetic field improves the strength of $\vec{v} \times \vec{B}$ force exerted on the electron, and increases the electron energy gain. After attaining the maximum energy gain, it is saturated for larger distances. It is because of the setting of betatron oscillations between the electron and the electric field of the laser pulse which enforces the electron to retain maximum energy even after passing of laser pulse. One can clearly see from fig. 5.4(a) and 5.4(b) that the electron retains high energy for larger distance in the presence of frequency chirp. In the absence of chirping the electron gains and retains relatively lower energy for relatively smaller distance than that in the presence of chirped laser pulse. Fig. 5.4(c) shows the variation of energy gain γ with z' for the different values of intensity parameter $a_0 = 6$, 7.5, 10, 12.5, 15, and 20 at $p_0' = 1.5$. The optimum values of magnetic field b_0 are derived from fig. 5.3(c) and the chirp parameter are same as taken in fig. 5.3(c). With the optimum value of magnetic field, initial momentum and suitable chirp parameter, the electron gains higher energy. It is clear that the higher energy gain is observed with higher values of laser pulse intensity. An acceleration gradient of the order of GeV/m was observed by Galow *et al.* [108] by using CP laser pulse with axial magnetic field of about $60T$. We employ an azimuthal magnetic field of about $9.4T$ with CP chirped laser pulse in vacuum to attain the same order of acceleration gradient.

Figure 5.5, shows the variation of acceleration gradient as a function of distance z. The acceleration gradient [108] can be obtained by using relation $d\gamma / dz = -e\vec{\beta}.\vec{E} / \beta_z$

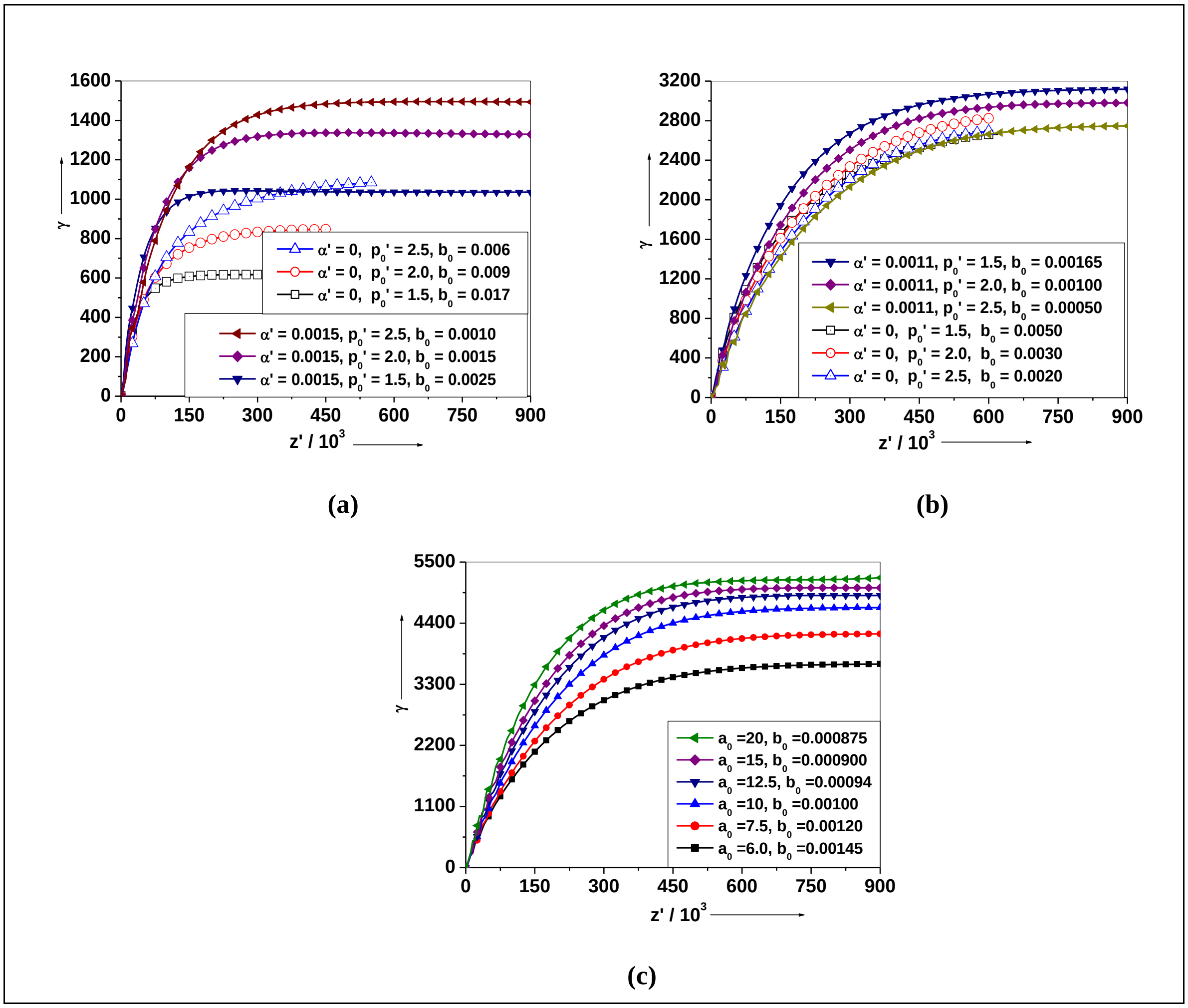

Figure 5.4. Energy gain γ with normalized distance z' for different values of normalized initial momentum p_0' and intensity parameters a_0 for CP laser pulses. (a) $p_0'=1.5$, 2, and 2.5 at $a_0=2.5$ with $\alpha'=0$ and $\alpha'=0.0015$, (b) $p_0'=1.5$, 2 and 2.5 at $a_0=5$ with $\alpha'=0$ and $\alpha'=0.0011$, and (c) $a_0=6$, 7.5, 10, 12.5, 15, and 20 at $p_0'=1.5$ with $b_0=0.00145$, 0.0012, 0.001, 0.00094, 0.0009, and 0.000875 and $\alpha'=0.000975$, 0.00088, 0.00078, 0.000725, 0.00069, and 0.00065 respectively. Rest parameters are same as taken in fig. 5.2.

and is plotted with distance z for a CP chirped laser pulse for different values of intensity parameter $a_0=2.5$, 5, 10, and 20 with normalized initial momentum $p_0'=1.5$ and

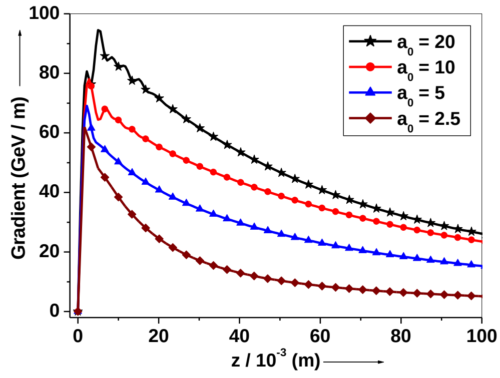

Figure 5.5. Electron acceleration gradient as a function of distance z for CP laser pulse with intensity parameter $a_0 = 2.5$, 5, 10, and 20 for $p_0' = 1.5$ and optimum values of magnetic field and chirp parameters. Rest parameters are same as taken in fig. 5.2.

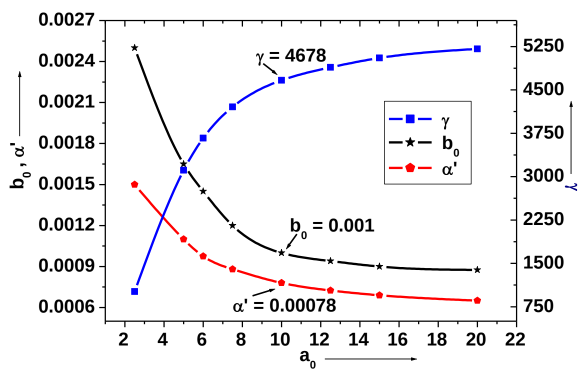

Figure 5.6. Electron energy gain γ calibration curve for normalized magnetic field b_0, chirping parameter α' and normalized energy gain γ as a function of normalized intensity a_0. Rest parameters are same as taken in fig. 5.2.

magnetic field and chirp parameter are found 0.001 (corresponding to a magnetic field of $106 kG$) and 0.00078 respectively. The optimum values of magnetic field and chirping factor decreases for attaining higher energy gain at high intensity. However, in order to attain maximum energy gain of $2.4 GeV$ at $a_0 = 10$ (corresponding to laser intensity $I \sim 2.74 \times 10^{20}\ W/cm^2$), the optimum values of optimum values of magnetic field b_0 as derived from fig. 5.3 and suitable chirp parameter α are same as taken in fig. 5.3. Sohbatzadeh *et al.* [59] reported an acceleration gradient of $59 GeV/m$ using a chirped femtosecond laser pulse with intensity $10^{19} W/cm^2$. However, we have observed an acceleration gradient of about $62 GeV/m$ with $a_0 = 2.5$ (corresponding to laser intensity $I \sim 1.7 \times 10^{19}\ W/cm^2$). Higher acceleration gradient is seen with higher values of laser intensity parameter. Further the emittance and radiative loss remains small with higher intensity pulses, as the radiative loss is not much with the pre accelerated electron [44]. The final momentum of emitted electron with maximum energy gain is related with emittance angle θ. Using relation $\tan\theta = (p_x^2 + p_y^2)^{1/2} / p_z$ with Lorentz factor, the angle of emittance with respect to z axis can be written as $\theta = \tan^{-1}(\sqrt{((\gamma^2 - 1)/\gamma^2 \beta_z^2) - 1}$. For energy gain of $1.5 GeV$ with $a_0 = 5$, the angle of emittance is 0.84° and for energy gain of $2.66 GeV$ with $a_0 = 20$ the angle of emittance is 0.64°. The obtained values of angle of emittance remain small for higher energy gain.

Figure 5.6, shows the electron energy gain γ calibration curve. The figure exhibits the variation of normalized magnetic field b_0, chirp parameter α' and energy gain γ as a function of intensity parameter a_0 with $p_0' = 1.5$.

The presented single particle simulations are supported by many particle simulations also. However, the exit energy gain for an ensemble of electrons is slightly different from that for single electron acceleration [96]. It is because of the Coulomb electron-electron interactions. The mean exit energy gain remains same with and without considering electron-electron interactions [108]. For an ensemble of electrons the polarization state and initial characteristics of electrons play important role in the acceleration of electron with a chirped laser pulse in vacuum. CP laser pulse can efficiently accelerate the electrons of a poor quality electron bunch [96] with very low energy spread. Thus the presented model of electron acceleration by CP chirped laser pulse in the presence of azimuthal magnetic field holds equally effective for an ensemble of particles.

5.5 CONCLUSION

Present study highlights the importance of CP chirped laser pulse and azimuthal magnetic field to obtain high electron energy gain in vacuum. We have observed an energy gain of $\gamma = 5210$ (corresponding to $2.66 GeV$) for laser intensity $a_0 = 20$ (corresponding to $2.74 \times 10^{20} W/cm^2$) with chirp parameter $\alpha' = 0.00065$ in the presence of azimuthal magnetic field $b_0 = 0.000875$ (corresponding to $94 kG$). Thus, a pre-accelerated electron of few MeV of initial energy can be accelerated up to GeV energy with optimized laser and magnetic field parameters as we have analysed in the present study.